SFRPs act as negative modulators of ADAM10 to regulate retinal neurogenesis

Pilar Esteve, Africa Sandonis, Marcos Cardozo, Jordi Malapeira, Carmen Ibanez, Inmaculada Crespo, Severine Marcos, Sara Gonzalez, Maria Luisa Toribio, Joaquin Arribas, et al.

SFRPs act as negative modulators of ADAM10 to regulate retinal neurogenesis

Pilar Esteve[1,2,3*], Africa Sandonìs[1,2,3], Marcos Cardozo[1,2,3], Jordi Malapeira[4a,b,c], Carmen Ibañez[1], Inmaculada Crespo[1,2,3], Severine Marcos[1,2,3], Sara Gonzalez-Garcia[1], Maria Luisa Toribio[1], Joaquin Arribas[4a,b,c], Akihiko Shimono[5], Isabel Guerrero[1] and Paola Bovolenta[1,2,3*]

[1]Centro de Biología Molecular "Severo Ochoa", CSIC-UAM , [2]CIBER de Enfermedades Raras (CIBERER), c/ Nicolas Cabrera, 1, Madrid 28049, Spain. [3]Instituto Cajal, CSIC Avda. Doctor Arce 37 28002 Madrid, Spain. [4a]Vall d'Hebron Institute of Oncology (VHIO), Psg. Vall d'Hebron 119-129, 08035 Barcelona, [4b]Department of Biochemistry and Molecular Biology, Universitat Autònoma de Barcelona, Campus de la UAB, 08193 Bellaterra, [4c]Institució Catalana de Recerca i Estudis Avançats (ICREA), 08010 Barcelona, Spain. [5]Cancer Science Institute of Singapore, National University of Singapore, Singapore 117456

Running title: Sfrp as modulators of ADAM function

***Correspondence to**: Paola Bovolenta
CBMSO, CSIC-UAM
Tel: +34 91 196 4718
Fax: +34 91 196 4420
e-mail: pbovolenta@cbm.uam.es

Pilar Esteve
CBMSO, CSIC-UAM
Tel: +34 91 196 4718
Fax: +34 91 196 4420
e-mail: pesteve@cbm.uam.es

It is well established that embryonic mouse retinal neurogenesis requires Notch signaling activation but is independent of the Wnt signaling pathway. Surprisingly, we show here that genetic inactivation of Sfrp1 and Sfrp2, two postulated Wnt antagonists, perturbs retinal neurogenesis. We solved this apparent paradox by demonstrating that in Sfrp1$^{-/-}$;Sfrp2$^{-/-}$ embryonic retinas, Notch signaling is transiently upregulated because Sfrps bind and downregulate ADAM10 metalloprotease activity, a critical step in Notch activation. Consistently, the proteolysis of other ADAM10 substrates, including APP, is altered in Sfrp mutants, whereas pharmacological ADAM10 inhibition partially rescues the Sfp1/2 null retinal phenotype. Conversely, ectopic Sfrp1 expression in the *Drosophila* wing imaginal disc prevents Notch targets' expression, which is completely restored by the co-expression of Kuzbanian, the Drosophila ADAM10 homolog. Together these data support a novel function for Sfrps as inhibitors of the ADAM10 metalloprotease, which might have important implications in pathological events, including cancer and Alzheimer disease.

During embryonic development, Notch and Wnt signaling orchestrate cell proliferation and cell fate decisions in a wide variety of tissues. The functional relationship between the two signaling pathways is intricate, and complementary or mutually exclusive activation has been reported, for example, during myogenesis, haematopoiesis or neurogenesis of the telencephalon or neural tube[1].

Notch and Wnt signaling are also required for the development of vertebrate neural retina. This structure develops from a neuroepithelium composed of multipotent progenitors, which undergo a series of competence states to give rise to six neuronal and one glial cell types[2]. As progenitor cells produce the various cell types, Notch through lateral inhibition, maintains neighboring cells in a multipotent, proliferative state, ensuring that sufficient numbers of progenitors are retained for consecutive waves of neurogenesis. Thus, downregulation of Notch is a prerequisite for retinal neuronal differentiation[2].

Wnt/βcatenin signaling has also been implicated in the proliferation of vertebrate retinal precursors. However, in the mouse embryonic neural retina this function is limited to progenitor cells located in the periphery[3, 4]. In contrast, Wnt/βcatenin signaling is not active in the central retina and cell proliferation and differentiation proceed normally in mice with conditional deletion of βcatenin in the neural retina, although retinal lamination is altered[5]. Similarly, retinal specific inactivation of Fzd5, a non-canonical Wnt receptor mostly impacts on retinal vasculature formation but has no effect on neurogenesis[6]. Despite this poor

implication of Wnt signaling in retinal differentiation, *Sfrp1* and *Sfrp2*, two members of a family of postulated Wnt antagonists, are strongly expressed in the neural retina throughout neurogenesis[7], raising the question of whether their function is related to Wnt signaling.

Sfrps, 1–5 in mammals, compose a family of secreted factors that fold in two independent domains. The Cystein Rich Domain (CRD) at the N–terminus shares similarities with the extracellular domain of the Wnt receptors Frizzled (Fzd) and ROR[8]. The C-terminal domain contains instead a Netrin-Related motif (NTR), which characterizes a number of unrelated proteins including Netrin–1, tissue inhibitors of metalloproteinases (TIMPs), complement proteins and TypeI procollagen C-proteinase enhancer proteins (PCOLCEs)[8]. Due to their homology to the extracellular portion of Fzd receptors, Sfrps were first described and mostly accepted as Wnt antagonists that bind and sequester Wnt ligands, thereby preventing signal activation. Gain of Sfrp1 or Sfrp2 function has proven especially useful to support this idea, as their excess of function antagonize Wnt signaling in a variety of contexts[8]. Loss of Sfrp function instead bespoke for two additional important features. First, Sfrp function might be redundant, because genetic inactivation of individual family members in mice seems to have little effect on embryonic development[9,10]. Double inactivation of *Sfrp1* and *Sfrp2* causes instead a variety of alterations[9, 11, 12], some of which are worsened by the additional inactivation of *Sfrp5*[9, 11]. Second, Sfrps have Wnt–independent functions[9,12] because Sfrp null phenotypes are only partially explained by overactivation of Wnt/βcatenin signaling[11] or alterations in the non–canonical Wnt/PCP pathway. Consistent with this notion, several studies have implicated individual Sfrps in the Wnt–independent regulation of other cell signaling mechanisms. For example, Sfrp1 can interact with and inhibit the activity of RANKL, a member of the TNF family involved in osteoclast formation[8]. Sfrp2 instead specifically binds to Tolloid metallo–proteinases and thereby regulates procollagen processing during myocardium infarction[13, 14]. Sfrp2 has also been described to interact with an integrin-fibronectin complex modulating apoptosis[8]. Furthermore, Sizzled a member of the family not present in mammals, acts as a negative feedback regulator of BMP signaling by binding to BMP1/Tolloid, a metalloprotease that normally degrades the Bmp antagonist chordin [15];[16].

By analyzing the functional consequences of *Sfrp1* and *Sfrp2* compound inactivation during mouse retinal neurogenesis, we demonstrate here a novel and Wnt–independent role of Sfrps in the regulation of Notch signaling. We explain this finding by demonstrating that Sfrps can bind and downregulate the activity of ADAM10, a metalloprotease with multiple substrates including Notch, N–cadherin and APP.

RESULTS

Sfrp1 and Sfrp2 are essential for proper eye development

Sfrp1 and *Sfrp2* are expressed during murine eye development with a complementary pattern that includes all eye structures[7]. *Sfrp1* transcripts are localized to the optic cup periphery and the retina pigmented epithelium from E10.5, while *Sfrp2* is predominant in the neural retina (**Fig. S1**). Despite restricted mRNA expression, Sfrp proteins efficiently diffuse in the extracellular space[17] and Sfrp1 was immunodetected, albeit at low levels, also in the neural retina (**Fig. S1**), supporting the proposed Sfrp functional redundancy[9, 11, 12]. Accordingly, the eye of *Sfrp1* and *Sfrp2* single null embryos appeared histologically normal. In contrast at E16.5, the latest viable stage, the eyes of *Sfrp1*$^{-/-}$*;Sfrp2*$^{-/-}$ compound mutants (*n=20*) were smaller than those of control littermates (*n=30*) with morphological visible alterations, including dorsal peripheral defects, reduction of the lens size, abnormal cornea and eye lid formation, increased thickness of the neural retina and abnormal vitreal accumulation of mesenchyme-derived angioblasts that normally form the hyaloid artery, the major vascular structure of the embryonic eye (**Fig. S2**).

Inactivation of *Sfrp1/2* alters retinal neurogenesis

Multipotent progenitors in the neural retina generates neuronal and one glial cells with an established temporal order. Retinal ganglion cells (RGCs) followed by amacrine and cone photoreceptors are the first cell types to be generated while bipolar and Müller glial cells are the last[2]. Although Wnt signaling does not appear to participate in retinal neurogenesis[4, 5] the neural retina of *Sfrp1*$^{-/-}$*;Sfrp2*$^{-/-}$ embryos was abnormally thick and with vascular defects, as determined by immunohistochemistry with endothelial and pericyte specific markers (**Fig. S2**). At E16.5, the number of Islet1–, Pax6–positive RGC, Islet1– and Pax6–positive amacrine cells as well as of Otx2–positive early born photoreceptors (74±5.72 vs 52±3.70 in controls) was increased in the neural retina of *Sfrp1*$^{-/-}$*;Sfrp2*$^{-/-}$ whereas PKCα–positive bipolar progenitors were virtually absent (2.33±0.408 vs 29±3.417 in controls), when compared to control retinas (**Fig. 1a**–**h**,**s**).

This increased differentiation of *Sfrp1/2* null retinas was not due to a premature onset of cell differentiation because no Tuj1–positive differentiating neurons were detected in either control or mutant retina at E10.5 (not shown). However, half a day later Tuj– and Islet1/2–positive mutant RGCs clearly outnumbered those of control retinas (**Fig. 1i**–**l**). This difference

was associated to a marked increase in BrdU-positive proliferating cells, which was already evident in the neural retina of E10.5 *Sfrp1*$^{-/-}$;*Sfrp2*$^{-/-}$ embryos when compared to control littermates (**Fig. 1m**,**n**,**s**). Furthermore, the distribution of E10.5 *Sfrp1*$^{-/-}$;*Sfrp2*$^{-/-}$retinal cells during the cell cycle using flow cytometry–based DNA content analysis revealed an increased distribution in the G2/M phase (G_1: 55%; S: 29.3%; G_2: 6.58%) when compared to that of littermates (G_1:51.8%; S:30.4 %; G_2:3.08%). This increase was only transient because at E16.5 the number of BrdU–positive cells was significantly reduced in the *Sfrp1*$^{-/-}$;*Sfrp2*$^{-/-}$ retinas as compared with controls (**Fig. 1q**,**r**,**s**).

Thus, Sfrp1/2 inactivation seemed to force the generation of progenitor cells and their differentiation into early born neurons, possibly depleting the proliferating progenitor pool with a consequent reduction of late born cell types.

Sfrp1/2 inhibits Notch signaling

The number of progenitor cells available for neural differentiation at any given time is controlled by Notch signaling[2]. To search for a Wnt–independent mechanism that could explain the neural retina phenotype of Sfrp mutants, we asked whether the Notch pathway was normally activated. Upon ligand binding, the Notch receptor becomes susceptible to two sequential proteolytic cleavages that enable the release of an active intracellular form of Notch (NICD). NICD translocates to the nucleus where it interacts with the CSL transcription factor and recruits co-activators to turn on the expression of Notch target genes, such as *Hes5*[18]. Nuclear localization of NICD is then a reliable determinant of Notch signaling activation[18].

In E12.5 control retinas, the number of NICD–positive progenitor cells available for neural differentiation occupied only a reduced central region[19] (**Fig. 2a**) whereas in the Sfrp1/2 mutants a significantly larger number of NICD-positive cells were distributed in most of the neural retina (**Fig. 2b**,**k**). With time, this difference became progressively inverted: at E13.5 the number of NICD-positive cells was similar in both control and mutant retinas but by E16.5 mutant retinas tended to contain fewer NICD positive cells as compared to control retinas (**Fig. 2c**–**f**; **k**). Consistent with a broad activation of the Notch pathway, the distribution of *Hes5* were similarly expanded in the *Sfrp1*$^{-/-}$;*Sfrp2*$^{-/-}$retinas (**Fig. 2g**,**h**) while those of the Notch ligand Delta-like1 (*Dll-1*), which is repressed upon Notch signaling activation[18] were abnormally low in the mutant neural retina (**Fig. 2i**,**j**). Q-RT-PCR analysis of *Hes5* (0.90±0.11 mutants vs 0.41±0.007 controls; $n=3$ $^*P<0.05$) and *Dll-1* (0.602±0.052 mutant vs 0.81±0.048 controls; $n=3$ $^*P<0.05$) mRNA levels from E13.5 control and Sfrp KO

retinas confirmed these variations. Together these data indicated that, in absence of Sfrp1/2, Notch signaling was abnormally active in a larger number of retinal progenitors explaining the early increase in cell proliferation. In turn, this simultaneous activation suppressed ligand expression, prematurely terminated retinal progenitor proliferation and favored their differentiation, explaining the accumulation of early differentiating neurons in *Sfrp*-null retinas.

We reasoned that if Sfrps directly or indirectly down–regulates Notch activity, similar alterations should occur in other brain regions where Notch and Sfrp1/2 are co–expressed, such as for example the telencephalon[20, 21]. Indeed, Western blot analysis of E12.5 *Sfrp1*$^{-/-}$*;Sfrp2*$^{-/-}$ and control cortex revealed that Notch was expressed at similar levels in both extracts but the NICD amount was fourfold higher in the mutants (**Fig. 2l**). This increase was paralleled by defects in telencephalic neurogenesis similar to those observed in the retina (I. Crespo, P. Bovolenta and P. Esteve, unpublished observations).

ADAM10 inhibition rescues the Sfrp KO retinal phenotype

The disintegrin and metalloprotease transmembrane protein ADAM10 is responsible for the first proteolytic cleavage that the Notch receptor suffers upon ligand binding[22 , 23]. ADAM10–mediated shedding of the Notch ectodomain is a limiting step for the subsequent proteolysis by the γ–secretase/presinilin complex, which releases the NICD. ADAM10 has been shown to be inhibited by tissue inhibitor of metalloproteases (TIMPs)[24] through the activity of their NTR module[24, 25]. Because Sfrp1/2 contain an NTR module[8], we postulated that Sfrp1/2 may normally down–regulate the activity of ADAM10. If this were the case, inhibition of ADAM10 activity should counteract the impaired neurogenesis observed in the *Sfrp1*$^{-/-}$*;Sfrp2*$^{-/-}$ neural retina.

G1254023X is a synthetic compound that inhibits ADAM10 with high affinity[26]. We thus examined its effect on retinal neurogenesis using organotypic optic cup cultures from E11.5 controls and *Sfrp1*$^{-/-}$*;Sfrp2*$^{-/-}$ embryos. After 24 h, culture conditions and treatment with vehicle (DMSO) alone did not significantly modified the difference in the rate of proliferation (measured by the number of BrdU positive cells) or differentiation (number of Islet1–positive cells) observed *in vivo* between control and *Sfrp1*$^{-/-}$*;Sfrp2*$^{-/-}$embryonic retinas (compare **Fig. 1s** with **Fig. S3** and **Fig. 3m**, **n**). Addition of G1254023X to the culture medium of control retinas reduced the rate of cell proliferation when compared to vehicle–treatment (**Fig. S3**). Exposure of *Sfrp1*$^{-/-}$*;Sfrp2*$^{-/-}$ optic cups to low concentrations of G1254023X was sufficient to reduce the number of BrdU-positive cells to values statistically undistinguishable from those

of controls (**Fig. 3a**,**c**,**i**). Increasing G1254023X concentrations (5μM) however further reduced the number of BrdU positive cells in *Sfrp1/2* null retinas to values below those of control retinas, supporting the idea that normally Sfrp1/2 negatively modulate but do not completely block Notch processing. Notably, G1254023X did not significantly change the number of Islet1–positive cells observed in the *Sfrp1*$^{-/-}$*;Sfrp2*$^{-/-}$ optic cup cultures at low doses but at higher concentrations favored cell differentiation (**Fig. 3e**–**h**,**j**). Likely, down–regulation of ADAM10 at a time when a significant amount of early born neurons has been already generated (**Fig. 1l**,**s**) is not sufficient to restrain cell cycle exit in the mutants. Rather, further inhibition of Notch activation promotes neuronal differentiation, as already reported in the retina[2].

Sfrps interfere with the proteolysis of ADAM10 substrates

Together the above findings supported the possibility that the *Sfrp1*$^{-/-}$*;Sfrp2*$^{-/-}$ retinal phenotype could be at least in part explained by an uncontrolled ADAM10 activity. We next postulated that, if this was the case, the processing of physiological ADAM10 substrates other than Notch should be equally altered in Sfrp null retinas.

ADAM10 sheds the extracellular domain of N–cadherin and L1–CAM, two cell adhesion molecules abundantly expressed in the embryonic retinas. This proteolytic cleavage produces fragments of 40kDa and 32kDa, respectively and is pre-requisite for further proteolysis by a γ–secretase, which generates intracellular peptides of 35kDa for N–cadherin[27] and 28kDa for L1–CAM[28]. Western–blot analysis of extracts from E13 and E16.5 *Sfrp1*$^{-/-}$*;Sfrp2*$^{-/-}$ and control retinas showed that the amount of L1–CAM 32kDa and N–cadherin 35kDa peptides were almost doubled in the mutants (70% and 68% of control values, respectively), although both proteins were expressed at similar levels in both genotypes (**Fig. 4a**,**b**). Consistent with the latter observation, membrane–bound active βcatenin, which requires intact N–cadherin to tether the membrane[27] was almost undetectable in the mutant retinas (**Fig. 4c**,**d**).

In addition to neural development, ADAM10 is crucial for tissue homeostasis. Most notably ADAM10 is responsible for the non amyloidogenic processing of Amyloid Precursor Protein (APP), a key protein in the onset of Alzheimer disease. ADAM10–mediated processing of APP cleaves the protein within the βamyloid peptide, preventing its toxic generation and promoting the shedding of a large soluble APP ectodomain[29] (sAPPα). APP is poorly expressed in developing retina (not shown) but its intact and sAPP forms are quite abundant in the subventricular zone of the lateral ventricle in adult mice[30]. If Sfrp1 normally antagonizes the ADAM10 α-secretase activity, sAPPα should be enriched in the lateral

ventricle of adult *Sfrp1*$^{-/-}$ mice. Comparative Western blot analysis of isolated lateral ventricle regions from *Sfrp1*$^{-/-}$ and wt brains confirmed an eightfold increase of sAPP levels in the mutants (**Fig. 5a**).

sAPPα is constitutively released from the surface of most cultured cells. Consistently, the amount of sAPPα recovered from *Sfrp1*, but not *Sfrp2*, stably transfected CHO cells was significantly reduced (47%) compared to control mock transfected CHO cells, although APP was expressed at similar levels in all the cell lines (**Fig. 5b**). Similarly addition of soluble recombinant Sfrp1, but not Sfrp2, significantly reduced (35%) the levels of sAPPα recovered from the media of CHO cells (**Fig. 5c**), further demonstrating that Sfrp1 is a specific inhibitor of ADAM10–mediated APP processing. The difference observed between Sfrp1 and Sfrp2 on APP processing raise also the possibility that Sfrps' inhibitory specificity may be influenced by the nature of the substrate, as also shown for other TIMPs[31].

Altogether these data indicate that Sfrp1, and likely Sfrp2, act as ADAM10 specific TIMPS.

Sfrp1 and ADAM10 physically interact

TIMPs usually exert their action by binding to their target metalloproteases[31]. To test whether Sfrps acted with a similar mechanism, we asked if Sfrp1 and ADAM10 physically interact. To this end we attempted to co-immunoprecipitate Sfrp1 and ADAM10 from embryonic retinal as well as from cortical tissue, where Sfrp1 is more abundantly expressed.

Indeed, Sfrp1 specific antibodies immunoprecipitated ADAM10 from wt but not from *Sfrp1*$^{-/-}$*;Sfrp2*$^{-/-}$tissues (**Fig. 6a**). Unfortunately in our hands, ADAM10 antibodies were not efficient in reverse immunoprecipitation experiments. To circumvent this problem, we cotransfected Sfrp1–HA and ADAM10–myc constructs in 293T cells and the derived cell lysates were analyzed to demonstrate that anti–myc antibodies specifically co–immunoprecipitated Sfrp1–HA with ADAM10 (**Fig. 6b**). Furthermore, secreted AP-tagged Sfrp1 appeared to bind on ADAM10 over-expressing CHO cells more abundantly than on the mock transfected cells that constitutively express low ADAM10 levels[31] (**Fig. 6c–f**).

Sfrp1 targets ADAM10 function independently of Wnt

The above findings strongly support that Sfrps can bind and directly modulate ADAM10 function. However, the partial rescue of the Sfrp phenotype by an ADAM10 inhibitor together with the notion that, in different contexts, Wnt and Notch activities are tightly linked,

prompted us to further ascertain whether Sfrps down–regulate ADAM10 independently of Wnt signaling.

To this end we turned to the *Drosophila* wing imaginal disc, the development of which is regulated by both Wnt and Notch signaling. In contrast to the vertebrate retina, the interaction between these two pathways, as well as their direct and specific down–stream targets have been unequivocally identified in *Drosophila*[32]. *Drosophila* offers also a natural Sfrp null background because no apparent Sfrp homolog has been identified in its genome[8]. Nevertheless, wingless efficiently binds to Sfrp1[33] mimicking vertebrate Wnt1 or Wnt8 interaction[34].

Taking advantage of this interaction, in a parallel study (Esteve et al., 2010, submitted), we have shown that HhGal4>UAS–Sfrp1 ectopic expression of Sfrp1 in the posterior compartment of the *Drosophila* wing imaginal disc interferes with the symmetrical gradient of wingless at the dorso-ventral boundary of the wing imaginal disc and thus prevents, in the posterior but not in the anterior compartment that serves as control, the expression of Senseless (Sens), a canonical target normally activated by high wingless levels in two discrete and symmetrical stripes at the dorso-ventral compartment boundary[35] (**Fig. 7a**,**b**). We thus asked if Sfrp1 could similarly interfere with the expression of genes directly activated by Notch signaling. Cut, one of such targets, is symmetrically expressed within the stripes of Sens at the dorso-ventral compartment boundary[32]. In the HhGal4>UAS–Sfrp1 wing discs Cut expression was totally abolished in the posterior but not in the anterior compartment (**Fig. 7c**), supporting that Sfrp1 interferes with Notch signaling. Consistently, the wing of adult UAS-myc-Sfrp1>Hh–Gal4 flies presented notches in the posterior wing margin, a phenotype characteristic of alterations in the wingless and Notch pathway (**Fig. 7e**,**f**). Most notably, forced expression of Kuzbanian (Kuz) (the *Drosophila* ADAM10 homolog) together with Sfrp1 in the posterior compartment completely rescued Cut expression, whereas had no effect on that of the wingless target Sens (**Fig. 7d**).

Together these results strongly support that Sfrp1 targets ADAM10/Kuz function, thus interfering with Notch signaling independently of Wnt.

DISCUSSION

The onset and progression of neurogenesis in the vertebrate retina is regulated by the interaction of the Fgf, Shh, Wnt and Notch signaling pathways. Comparison of the mechanisms operating in different species offers two important observations. First, there are species–specific differences in the precise composition and onset of each pathway, which reflect individual retinal characteristics[36]. Second individual elements of one pathway respond or are used in other signaling cascades or cellular activities. For example in the eye, Hes1, an established Notch target, is also independently regulated by Shh and Wnt signaling[37, 38], and β–catenin, a key element of Wnt signaling, has a well characterized function in cell-cell adhesion[5]. In this study we show that Sfrps, accepted modulators of Wnt signaling, unexpectedly act as negative regulators of Notch. This novel Sfrp function provides an additional example of how individual molecules are shared by different signaling cascades. Mechanistically, Sfrps bind and, independently of Wnt, down–regulate the α–secretase activity of ADAM10, which is responsible for the proteolytic cleavage of the Notch receptor and thus of the subsequent pathway activation[23]. Furthermore, by targeting ADAM10, Sfrps regulate the proteolysis of other specific substrates, including N–Cadherin, L1–CAM and APP.

These conclusions stem from the initial observation that in *Sfrp1*$^{-/-}$*;Sfrp2*$^{-/-}$ embryos the periphery of the optic cup is not specified and the neural retina is abnormally thick. Specification of the optic cup periphery depends on Wnt signaling activation[3, 4]. In a parallel study, we showed that Sfrp1/2 proteins are required to activate canonical signaling in the periphery of the optic cup, likely promoting the diffusion of Wnt ligands (Esteve et al., 2010, submitted). This mechanism however could not explain the transient increase in proliferation and the enhanced generation of early born neurons in the *Sfrp1*$^{-/-}$*;Sfrp2*$^{-/-}$ neural retina, because previous studies had convincingly demonstrated that Wnt signaling does not significantly contribute to retinal neurogenesis in mice[5,6]. We also considered unlikely that the retinal phenotype could be secondary to the vascular defects observed in Sfrp1/2 null mice, because neurogenesis proceeds normally in embryos where the hyaloid artery does not form[39]. Instead, we demonstrated that abnormal retinal neurogenesis could be explained by a transient increase in Notch signaling likely caused by an enhanced ADAM10 activity. Supporting this interpretation, we showed that pharmacological inhibition of ADAM10 can rescue the enhanced cell proliferation of *Sfrp1*$^{-/-}$*;Sfrp2*$^{-/-}$ neural retina. Furthermore, conditional inactivation of *Adam10* in neural progenitor cells causes a depletion of early progenitors and a

reduction of α–secretase-mediated processing of APP[22], a phenotype opposite to that observed in *Sfrp1/2* null retinas or in the cortex of *Sfrp1*$^{-/-}$embryos (I. Crespo, P. Bovolenta and P. Esteve, unpublished observations), where Notch and APP processing is upregulated. Notably, similar defects characterize also the cortex of embryos deficient in RECK (reversion–inducing cysteine–rich protein with Kazal motifs), a membrane protein localized to cortical precursor cells, which is thought to inhibit ADAM10 sheddase activity but with Notch ligands as substrates[40].

Our analysis of Sfrp null ocular phenotype together with over–expression studies in the *Drosophila* wing disc strongly support that Sfrps independently modulate Wnt and Notch. Indeed Sfrp1 in the posterior compartment of the *Drosophila* wing imaginal disc interferes with the expression of Wnt and Notch target genes but co–expression of Sfrp1 and Kuz/ADAM10 completely rescue Notch but not wingless target expression. Therefore, when co–activated, these pathways may compete for Sfrp–mediated regulation, which provides an additional frame to interpret the reported functional interaction between Wnt/canonical and Notch signaling in several contexts[41].

The ADAM family of metalloprotease is quite large. Phylogenetic and functional analysis of the human members indicates that ADAM10 is closely related to ADAM17 but separated by other family members. The distribution of *Adam10* and *Adam17* largely overlaps and initial studies suggested that both metalloproteases participated in Notch and APP cleavage[42],[29]. Therefore, we cannot totally exclude that abnormal activity of ADAM17 might contribute to the ocular phenotype *Sfrp1/2* null mice. The existence of an Sfrp–mediated regulation of ADAM17 might, for example, contribute to explain why specific pharmacological inhibition of ADAM10 only partially rescue the retinal phenotype of *Sfrp1*$^{-/-}$*;Sfrp2*$^{-/-}$embryos. However, we favor the hypothesis that at least in the Central Nervous System Sfrp1 and 2 largely target ADAM10 function. Indeed, genetic inactivation in mice indicates that *Adam10* has a preponderant function in the developing central nervous and cardiovascular systems, whereas *Adam17* regulates epithelial maturation of multiple organs[42]. Furthermore, recent studies have convincingly demonstrated that at least in the CNS Notch, APP and N–cadherin are ADAM10 specific substrates[22, 43]. In line with these findings, we have demonstrated that the proteolytic processing of these three substrates, as well as that of L1–CAM, is altered in *Sfrp1/2* null mice. Notwithstanding, future studies based on the use of other tissues, where ADAM17 appears to be preponderant, should help to resolve the specificity of Sfrps on ADAM regulation.

Sfrp2 and Sizzled, a non–mammalian Sfrp family member, have been previously shown to regulate Tolloid metalloproteinases (also known as procollagen C–proteinases), but with different functions. In vertebrates, BMP activity is in part controlled by the BMP antagonist Chordin which, in turn, is inactivated through cleavage by Tolloid. Sizzled, but apparently not Sfrp2[13] binds to Tolloid and behaves as a TIMP acting as competitive inhibitor of the enzymatic activity, thus preventing Chordin cleavage[15];[16]. Sfrp2 instead interacts through its CRD to the non–protease domain of Tolloid proteases and enhances their procollagen–C proteinase activity[13] or inhibits it depending of its concentration[14]. The way by which Sfrp1, and possibly Sfrp2, inhibits ADAM10 is still unclear but may bear similarities with the above mechanisms.

Sfrps, TIMPs and PCOLCEs share similarities in the NTR domain which, in TIMP and POLCE is thought to interfere with protease activity[44]. The structure of ADAM10 comprises, adjacent to the catalytic and disintegrin domains, a cysteine–rich motif, which is thought to mediate interaction with other molecules[42]. In a plausible model (**Fig. S4**), binding of the respective cysteine–rich motifs may be responsible for Sfrp/ADAM interaction, which would bring the Sfrp NTR domain close to the ADAM10 catalytic site. Thus, Sfrp1/2 would interfere with ADAM10 enzymatic activity by competing for substrate binding. Given the molecular diversity of metalloprotease substrates, it is possible that the inhibitory specificity may be in part linked to the nature of the substrates, as suggested by the specific effect of Sfrp1 but not by Sfrp2 on APP processing. This possibility is supported by tissue distribution. In fact, APP and Sfrp1, but not Sfrp2, are particularly abundant in the telencephalon. In contrast, ADAM10–mediated processing of Notch in the retina seems to involve both Sfrp1 and Sfrp2.

Independently of the precise mechanism of action, the dual role of Sfrps in the regulation of Wnt signaling and ADAM10 activity might be relevant in different pathological situations, especially in neurodegenerative diseases or metastatic events, where both Wnt signaling components and metalloproteases play major roles[41]. For example ADAM10 confers metastatic capacity in colorectal cancer[45]. Loss of *SFRP1* and *SFRP2* expression due to promoter hypermethylation has been frequently observed in proliferating and invasive tumors of different nature [8]. Conversely, ectopic Sfrp1 expression inhibits tumor growth and lung metastasis induced by inoculation of invasive tumorigenic cell line[46], notably associated with changes in both Wnt/βcatenin and extracellular matrix components[46]. Thus, potentiating Sfrp1 activity might have the double function of controlling Wnt mediated tumor proliferation and ADAM mediated invasion.

On the contrary, our results point to the inhibition of Sfrp1 as a potential mechanism to prevent the toxic accumulation of Aβ peptides, one of the landmarks of Alzheimer disease. Indeed, in absence of Sfrp1 function, APP processing should shift toward the production of sAPPα, thus preventing the generation of Aβ, as recently shown for SIRT1, a deacetylase that directly activates the transcription of ADAM10[47]. Whether this would be beneficial to Alzheimer pathology is worth testing, although it is becoming apparent that the contribution of APP proteolytic derivatives to the Alzheimer pathology is more complex than what originally envisaged.

ACKNOWLEDGMENTS

We wish to thank Jose Maria Ruiz for help with some initial experiments and Isidro Dompablo for excellent technical assistance. We also thank H. Bellen, T. Tabata, S. Campuzano and DSHB for *Drosophila* antibodies and stocks and A. Ludwig for kindly providing the G1254023X compound. This work was supported by grants from the Spanish MICINN, BFU2007–61774, Fundación Mutual Madrileña (2006-0916), Comunidad Autonoma de Madrid (CAM, P–SAL–0190–2006), PIE–CSIC and CIBERER intramural funds to P.B.; CSIC intramural funds to P.E.; grants BFU2008–03320/BMC and CSD2007–00008 from the Spanish MICINN to IG and by an institutional grant from Fundación Areces given to the Centro de Biología Molecular "Severo Ochoa" to IG and MT.

Authors' contributions

PE and with ASa performed most of the immunohistochemical, ISH and Western blot analysis. ASh generated the Sfrp KO mice. MC and IC performed IP and binding assays. JM and JA designed and performed APP shedding experiments in CHO cells. IG designed and performed with CI the assays in *Drosophila*. SM contributed Sfrp1 and Sfrp2 ISH localization. SGG and MLT contributed expertise in Notch signaling and flow cytometry studies. PB and PE conceived and supervised the study and wrote the manuscript.

References

1. Hayward, P., Kalmar, T. & Arias, A.M. Wnt/Notch signalling and information processing during development. *Development* **135**, 411-424 (2008).
2. Livesey, F.J. & Cepko, C.L. Vertebrate neural cell-fate determination: lessons from the retina. *Nat Rev Neurosci* **2**, 109-118 (2001).
3. Cho, S.H. & Cepko, C.L. Wnt2b/beta-catenin-mediated canonical Wnt signaling determines the peripheral fates of the chick eye. *Development* **133**, 3167-3177 (2006).
4. Liu, H.*, et al.* Ciliary margin transdifferentiation from neural retina is controlled by canonical Wnt signaling. *Dev Biol* **308**, 54-67 (2007).
5. Fu, X., Sun, H., Klein, W.H. & Mu, X. Beta-catenin is essential for lamination but not neurogenesis in mouse retinal development. *Dev Biol* **299**, 424-437 (2006).
6. Liu, C. & Nathans, J. An essential role for frizzled 5 in mammalian ocular development. *Development* **135**, 3567-3576 (2008).
7. Liu, H., Mohamed, O., Dufort, D. & Wallace, V.A. Characterization of Wnt signaling components and activation of the Wnt canonical pathway in the murine retina. *Dev Dyn* **227**, 323-334 (2003).
8. Bovolenta, P., Esteve, P., Ruiz, J.M., Cisneros, E. & Lopez-Rios, J. Beyond Wnt inhibition: new functions of secreted Frizzled-related proteins in development and disease. *J Cell Sci* **121**, 737-746 (2008).
9. Satoh, W., Gotoh, T., Tsunematsu, Y., Aizawa, S. & Shimono, A. Sfrp1 and Sfrp2 regulate anteroposterior axis elongation and somite segmentation during mouse embryogenesis. *Development* **133**, 989-999 (2006).
10. Trevant, B.*, et al.* Expression of secreted frizzled related protein 1, a Wnt antagonist, in brain, kidney, and skeleton is dispensable for normal embryonic development. *J Cell Physiol* **217**, 113-126 (2008).
11. Satoh, W., Matsuyama, M., Takemura, H., Aizawa, S. & Shimono, A. Sfrp1, Sfrp2, and Sfrp5 regulate the Wnt/beta-catenin and the planar cell polarity pathways during early trunk formation in mouse. *Genesis* **46**, spcone (2008).
12. Misra, K. & Matise, M.P. A critical role for sFRP proteins in maintaining caudal neural tube closure in mice via inhibition of BMP signaling. *Dev Biol* **337**, 74-83.
13. Kobayashi, K.*, et al.* Secreted Frizzled-related protein 2 is a procollagen C proteinase enhancer with a role in fibrosis associated with myocardial infarction. *Nat Cell Biol* **11**, 46-55 (2009).
14. He, W.*, et al.* Exogenously administered secreted frizzled related protein 2 (Sfrp2) reduces fibrosis and improves cardiac function in a rat model of myocardial infarction. *Proc Natl Acad Sci U S A*.
15. Lee, H.X., Ambrosio, A.L., Reversade, B. & De Robertis, E.M. Embryonic dorsal-ventral signaling: secreted frizzled-related proteins as inhibitors of tolloid proteinases. *Cell* **124**, 147-159 (2006).
16. Muraoka, O.*, et al.* Sizzled controls dorso-ventral polarity by repressing cleavage of the Chordin protein. *Nat Cell Biol* **8**, 329-338 (2006).
17. Mii, Y. & Taira, M. Secreted Frizzled-related proteins enhance the diffusion of Wnt ligands and expand their signalling range. *Development* **136**, 4083-4088 (2009).
18. Kopan, R. & Ilagan, M.X. The canonical Notch signaling pathway: unfolding the activation mechanism. *Cell* **137**, 216-233 (2009).
19. Del Monte, G., Grego-Bessa, J., Gonzalez-Rajal, A., Bolos, V. & De La Pompa, J.L. Monitoring Notch1 activity in development: evidence for a feedback regulatory loop. *Dev Dyn* **236**, 2594-2614 (2007).

20. Tokunaga, A.*, et al.* Mapping spatio-temporal activation of Notch signaling during neurogenesis and gliogenesis in the developing mouse brain. *J Neurochem* **90**, 142-154 (2004).
21. Kim, A.S., Lowenstein, D.H. & Pleasure, S.J. Wnt receptors and Wnt inhibitors are expressed in gradients in the developing telencephalon. *Mech Dev* **103**, 167-172 (2001).
22. Jorissen, E.*, et al.* The disintegrin/metalloproteinase ADAM10 is essential for the establishment of the brain cortex. *J Neurosci* **30**, 4833-4844.
23. Hartmann, D.*, et al.* The disintegrin/metalloprotease ADAM 10 is essential for Notch signalling but not for alpha-secretase activity in fibroblasts. *Hum Mol Genet* **11**, 2615-2624 (2002).
24. Amour, A.*, et al.* The in vitro activity of ADAM-10 is inhibited by TIMP-1 and TIMP-3. *FEBS Lett* **473**, 275-279 (2000).
25. Langton, K.P., Barker, M.D. & McKie, N. Localization of the functional domains of human tissue inhibitor of metalloproteinases-3 and the effects of a Sorsby's fundus dystrophy mutation. *J Biol Chem* **273**, 16778-16781 (1998).
26. Ludwig, A.*, et al.* Metalloproteinase inhibitors for the disintegrin-like metalloproteinases ADAM10 and ADAM17 that differentially block constitutive and phorbol ester-inducible shedding of cell surface molecules. *Comb Chem High Throughput Screen* **8**, 161-171 (2005).
27. Reiss, K.*, et al.* ADAM10 cleavage of N-cadherin and regulation of cell-cell adhesion and beta-catenin nuclear signalling. *Embo J* **24**, 742-752 (2005).
28. Riedle, S.*, et al.* Nuclear translocation and signalling of L1-CAM in human carcinoma cells requires ADAM10 and presenilin/gamma-secretase activity. *Biochem J* **420**, 391-402 (2009).
29. Lichtenthaler, S.F. Alpha-secretase in Alzheimer's disease: molecular identity, regulation and therapeutic potential. *J Neurochem* **116**, 10-21.
30. Caille, I.*, et al.* Soluble form of amyloid precursor protein regulates proliferation of progenitors in the adult subventricular zone. *Development* **131**, 2173-2181 (2004).
31. Stetler-Stevenson, W.G. Tissue inhibitors of metalloproteinases in cell signaling: metalloproteinase-independent biological activities. *Sci Signal* **1**, re6 (2008).
32. Micchelli, C.A., Rulifson, E.J. & Blair, S.S. The function and regulation of cut expression on the wing margin of Drosophila: Notch, Wingless and a dominant negative role for Delta and Serrate. *Development* **124**, 1485-1495 (1997).
33. Uren, A.*, et al.* Secreted frizzled-related protein-1 binds directly to Wingless and is a biphasic modulator of Wnt signaling. *J Biol Chem* **275**, 4374-4382 (2000).
34. Lopez-Rios, J., Esteve, P., Ruiz, J.M. & Bovolenta, P. The Netrin-related domain of Sfrp1 interacts with Wnt ligands and antagonizes their activity in the anterior neural plate. *Neural Dev* **3**, 19 (2008).
35. Nolo, R., Abbott, L.A. & Bellen, H.J. Senseless, a Zn finger transcription factor, is necessary and sufficient for sensory organ development in Drosophila. *Cell* **102**, 349-362 (2000).
36. Esteve, P. & Bovolenta, P. Secreted inducers in vertebrate eye development: more functions for old morphogens. *Curr Opin Neurobiol* **16**, 13-19 (2006).
37. Wall, D.S.*, et al.* Progenitor cell proliferation in the retina is dependent on Notch-independent Sonic hedgehog/Hes1 activity. *J Cell Biol* **184**, 101-112 (2009).
38. Kubo, F. & Nakagawa, S. Hairy1 acts as a node downstream of Wnt signaling to maintain retinal stem cell-like progenitor cells in the chick ciliary marginal zone. *Development* **136**, 1823-1833 (2009).
39. Morcillo, J.*, et al.* Proper patterning of the optic fissure requires the sequential activity of BMP7 and SHH. *Development* **133**, 3179-3190 (2006).

40. Muraguchi, T.*, et al.* RECK modulates Notch signaling during cortical neurogenesis by regulating ADAM10 activity. *Nat Neurosci* **10**, 838-845 (2007).
41. Campbell, C., Risueno, R.M., Salati, S., Guezguez, B. & Bhatia, M. Signal control of hematopoietic stem cell fate: Wnt, Notch, and Hedgehog as the usual suspects. *Curr Opin Hematol* **15**, 319-325 (2008).
42. Edwards, D.R., Handsley, M.M. & Pennington, C.J. The ADAM metalloproteinases. *Mol Aspects Med* **29**, 258-289 (2008).
43. Kuhn, P.H.*, et al.* ADAM10 is the physiologically relevant, constitutive alpha-secretase of the amyloid precursor protein in primary neurons. *Embo J* **29**, 3020-3032.
44. Mott, J.D.*, et al.* Post-translational proteolytic processing of procollagen C-terminal proteinase enhancer releases a metalloproteinase inhibitor. *J Biol Chem* **275**, 1384-1390 (2000).
45. Gavert, N.*, et al.* Expression of L1-CAM and ADAM10 in human colon cancer cells induces metastasis. *Cancer Res* **67**, 7703-7712 (2007).
46. Matsuda, Y., Schlange, T., Oakeley, E.J., Boulay, A. & Hynes, N.E. WNT signaling enhances breast cancer cell motility and blockade of the WNT pathway by sFRP1 suppresses MDA-MB-231 xenograft growth. *Breast Cancer Res* **11**, R32 (2009).
47. Donmez, G., Wang, D., Cohen, D.E. & Guarente, L. SIRT1 suppresses beta-amyloid production by activating the alpha-secretase gene ADAM10. *Cell* **142**, 320-332.
48. Torroja, C., Gorfinkiel, N. & Guerrero, I. Patched controls the Hedgehog gradient by endocytosis in a dynamin-dependent manner, but this internalization does not play a major role in signal transduction. *Development* **131**, 2395-2408 (2004).
49. Tanimoto, H., Itoh, S., ten Dijke, P. & Tabata, T. Hedgehog creates a gradient of DPP activity in Drosophila wing imaginal discs. *Mol Cell* **5**, 59-71 (2000).
50. Rodriguez, J.*, et al.* SFRP1 regulates the growth of retinal ganglion cell axons through the Fz2 receptor. *Nat Neurosci* **8**, 1301-1309 (2005).

FIGURE LEGENDS

Figure 1. Neurogenesis is impaired in the central retina of *Sfrp1*$^{-/-}$;*Sfrp2*$^{-/-}$ embryos. Frontal cryostat sections of E16.5 (**a-h**, **q**,**r**), E12.5 (**o**,**p**), E11.5 (**i–l**) and E10.5 (**m**,**n**) control and *Sfrp1*$^{-/-}$;*Sfrp2*$^{-/-}$ retinas immunostained with antibodies against Tuj1 (differentiated cells), Islet1 (RGC and amacrine), Pax6 (RGC, amacrine) Otx2 (bipolar, photoreceptors) PKC (bipolar) and BrdU (proliferating precursors) and counterstained with DAPI (Blue, a–h and k–l). RGC and amacrine cells are increased, whereas bipolar cells are decreased in the mutant retinas. Proliferation rate in the mutant retinas is increased at early stages but is reduced at E16.5 as compared to controls (compare **r** to **q**). **s**) Quantification of BrdU+, Islet1+, Otx2+ and PKC+, cells. Positive cells were counted in equivalent areas of the central retina. Error bars are standard error of the mean (s.e.m.) of at least three sections from four different embryos (*n=4*). Abbreviations: rgc, retina ganglion cells; rpe, retina pigmented epithelium.**P*<0.05. ***P*<0.01. ****P*<0.001. Scale bar, 30μm (**a**–**l**, **q**,**r**), 60μm (**o**,**p**); 100μm (**m**,**n**).

Figure 2. Notch signaling is transiently upregulated in *Sfrp1*$^{-/-}$;*Sfrp2*$^{-/-}$ retinas. Frontal cryostat sections of E12.5 (**a**,**b**,**g**,**h**), E13.5 (**c**,**d**,**i**,**j**) and E16.5 (**e**,**f**) control and mutant embryos immunostained with antibodies against NICD (**a–f**) or hybridized with probes specific for *Hes5* (**g**,**h**) or *Dll-1* (**i**,**j**). Note the initial expansion of NICD and *Hes5* expression in the mutants (arrowheads in **g**,**h**). The expression of *Dll-1* is instead down-regulated. **k**) Quantification of the number of NICD+ cells in the neural retina. Positive cells were counted in equivalent areas. Error bars are s.e.m. of at least three sections. Four different embryos were analyzed in each case (*n=4*). **l**) Western blot analysis of the levels of Notch processing in lysates of E12.5 cortex from mutant and control embryos. Note that the cleaved Notch fragment (NICD) is increased in the mutants as determined by band intensity quantification normalized with α-tubulin (3.5 vs 1.2 in controls), although Notch is expressed at similar levels in both tissues (1.482 vs 1.46 in controls). The data represent a typical experiment, which was repeated four times with similar results. Scale bar: 30μm (**a-f**); 50μm (**i,j**); 100μm (**g,h**).

Figure 3. Inhibition of ADAM10 partially rescues the retinal phenotype of *Sfrp1/2* null embryos. Cryostat sections of organotypic optic cup cultures from E11.5 controls (**a**,**e**,**i**,**j**) or *Sfrp1*$^{-/-}$;*Sfrp2*$^{-/-}$ (**b–d**,**f–h**,**i**,**j**) embryos cultured for 24h in the presence of DMSO (**a**,**b**,**e**,**f**,**i**,**j**) or 1–5μM of the ADAM10 inhibitor G1254023X (**c**,**d**,**g**,**h**,**i**,**j**). Sections were immunostained

with antibodies against BrdU (**a**–**d**) or Islet1(**e**–**h**). **i**,**j**) Quantification of BrdU+, and Islet1+ cells. Positive cells were counted in equivalent areas of the central retina. Note that cultures retinas from *Sfrp1*$^{-/-}$*;Sfrp2*$^{-/-}$ embryos shows an increase in cell proliferation and differentiation similar to that observed in vivo. Addition of 1–2μM G1254023X is sufficient to decrease proliferation but not differentiation values to those of controls. Error bars are s.e.m of at least three sections from 5 different cultures (*n=5*). *,$^{\#}$*P*<0.05. **, $^{\#\#}$*P*<0.01. ***, $^{\#\#\#}$*P*<0.001. Asterisks indicate comparison between controls and GX–treated mutant cultures; # between DMSO– or G1254023X –treated mutant cultures. Scale bar: 30μm.

Figure 4. Sfrps interferes with ADAM10–mediated processing of N–cadherin and L1. Western blot analysis of L1 (**a**) and N–cadherin (**b**) processing in lysates of retinas from E13.5 and E16.5 mutant and control embryos. Note that the 32kDa L1 and 35kDa N–cadherin fragments (CTFs) are increased in *Sfrp1*$^{-/-}$*;Sfrp2*$^{-/-}$ mutants as determined by band intensity quantification normalized to α–tubulin (4.4 vs 2.58 in controls for L1, and 6.51 vs 3.86 in controls for N–cadherin) . The data represent a typical experiment, which was repeated three times with similar results. **c**,**d**) Increased N–cadherin processing is paralleled by loss of membrane bound active βcatenin in the mutant retinas as compared to controls. Abbreviations: rgc, retina ganglion cells; rpe, retina pigmented epithelium. Scale bar; 30μm.

Figure 5. Sfrps interferes with ADAM10-mediated processing of APP. a) Western blot analysis of total (APP) and soluble (sAPPα) present in lysates from the subventricular zone of the lateral ventricles from wt and *Sfrp1*$^{-/-}$ adult brains. The amount of sAPPα fragment is increased in mutants (Normalized density values to α–tubulin: 11.1 vs 1.32 in controls). The data represent a typical experiment, which was repeated three times with similar results. **b**) Western blot analysis of total (APP) and soluble (sAPPα) present, respectively, in the cell lysate and conditioned media of CHO cells stably transfected with *Sfrp2* or *Sfrp1* constructs (left column, densitometric analysis of sAPPα in the media normalized to ponceau stained vector: 10.9± 2.2 Sfrp2: 13.3± 0.7 Sfrp1: 5.2±1. 7) or **c**) of CHO cells incubated with purified Sfrp1 or Sfrp2 proteins, (densitometric analysis of sAPPα in the media normalized to ponceau stained vector: 10.0±1.6 Sfrp2: 11.8±0.7 Sfrp1: 4.1±2.2). Note that in both cases Sfrp1, but not Sfrp2, treatment decreases the amount of secreted APP without changing the levels of APP expression in the cell lysates.

Figure 6. Sfrps interacts with ADAM10. a) Embryonic telencephalic and ocular tissue from wt and Sfrp mutants were inmunoprecipitated with anti-Sfrp1 antibody and analyzed by Western blot with anti-ADAM10 antibody. Asterisks in the upper panel indicate the co-immunoprecipitation of ADAM10 in wt tissue. Asterisks in the middle panel indicate Sfrp1 in wt tissue. Asterisks in the bottom panel indicate ProADAM10 and ADAM10 bands. The data represent a typical experiment, which was repeated five times with similar results. **b**) HEK 293T cells were transiently transfected with expression plasmids of ADAM-myc, Sfrp1-HA or a combination of both. After 48h cell lysates were precipitated with anti-myc antibodies and analyzed by Western blot with anti-HA antibody. Note that ADAM10 can immunoprecipitate Sfrp1 (asterisk). The data represent a typical experiment, which was repeated five times with similar results. **c**–**f**) CHO cells were transfected with an ADAM10 expression plasmid or with the empty vector. Cells were thereafter incubated with conditioned media containing AP–Sfrp1 or AP alone. Increased binding AP-Sfrp1 is observed in the ADAM10 over-expressing cell line. Scale bar; 25μm.

Figure 7. Sfrp1 interacts with Kuz in *Drosophila* wing imaginal discs. **a**,**b**) Senseless (blue in a,b) and extracellular wingless expressions (red) in a UAS–myc-Sfrp1>Hh–Gal4 wing imaginal disc. Observe the repression of the wingless target Sens in the posterior compartment where Sfrp1 is expressed (Myc in green) but not in the anterior compartment that serves as a control. **c**) Cut (green) and Hh (red) expressions in Hh–Gal4>UAS–myc–Sfrp1 wing discs. Note the repression of the Notch target Cut (open arrowhead) in the area where Sfrp1 is expressed (Hh in red). **d**) Sens (blue) and Cut (green) expression in a UAS–myc–Sfrp1/UAS–Kuz>Hh–Gal4 wing disc (Myc in red). The ectopic expression of both Sfrp1 and Kuz rescues the expression of the Notch target Cut (arrowhead) but has no effect on that of the Wg target Sens. **e**) Adult UAS–myc-Sfrp1>Hh–Gal4 wing phenotype showing notches in the posterior wing margin, a phenotype characteristic of wingless and Notch signaling alterations. f) Wild type wing. Scale bar, 40μm (**a**–**d**); 200μm (**e**,**f**).

ONLINE METHODS

Animals: *Sfrp1*$^{-/-}$*;Sfrp2*$^{+/-}$ mutant mice were generated as described[9] and inter-crossed to generate *Sfrp1*$^{-/-}$*;Sfrp2*$^{-/-}$double mutant embryos. *Sfrp1*$^{-/-}$*;Sfrp2*$^{+/-}$ were mated with 129 and C57BL/6 mixed background to obtain *Sfrp1*$^{+/-}$*;Sfrp2*$^{+/-}$ double heterozygous strain and further used to generate single *Sfrp1* and *Sfrp2* mutant. The eyes of *Sfrp1*$^{-/-}$ and *Sfrp2*$^{-/-}$ single mutants were normal and undistinguishable from those of age matched wild types and therefore littermates were often used as controls for the double mutant embryos.

***Antibodies*:** We used the following primary antibodies: mouse monoclonal anti-Brdu (1:500, Boehringer Manheim), mouse monoclonal anti-Islet1 (1:500, Hybridoma Bank, 39.4D5); rabbit polyclonal anti-Otx2 (1:500, Abcam); rabbit polyclonal anti-Calbindin-28K (1:2000 Swant); mouse monoclonal anti-Active βcatenin (ABC) (1:200, Millipore), mouse monoclonal anti-Myc (1:2000, clone 9E10); rabbit polyclonal anti-Pax6 (1:500, Covance); mouse monoclonal anti-PKC (1:400, SIGMA-ALDRICH); mouse monoclonal anti-βIII-Tubulin (1:4000, Promega), rabbit polyclonal anti-cleaved Notch1 Val1744 (1:200, Cell signalling), goat polyclonal Notch 1 (Santa Cruz) rabbit polyclonal anti-HA (1:2000, SIGMA-ALDRICH), mouse monoclonal anti-HA (1:2000, SIGMA-ALDRICH), rabbit polyclonal anti-Myc (SIGMA-ALDRICH), mouse monoclonal anti-Amyloid Precursor Protein A4 (1:5000, Millipore, clone 22C11), rabbit polyclonal anti-soluble APPα (1:500, Covance) rabbit polyclonal anti-Sfrp1 (1:500 AbCam), rabbit polyclonal anti-NG2 (1:500, Chemicon), mouse monoclonal N-cadherin C-terminal domain (1:500, Zymed Laboratories, clon 3B9), rabbit polyclonal 74 5H7 to the cytoplasmic part of L1 (a gift of V.P. Lemmon), goat polyclonal anti-Adam10 (1:500 RD) guinea-pig anti-Sens[35] 1/1000 (a gift of H. Bellen), rabbit anti-Hh antibody (1/800; a gift of T. Tabata); mouse anti-Wg 1/50 and anti-Cut (prepared from cells obtained from the DSHB) and Lectin from Tomato biotin-conjugated (1:150, SIGMA-ALDRICH). Secondary antibodies: rabbit Alexa-488, rabbit Alexa-594, mouse Alexa -488 (1:2000 Molecular Probes).

***In situ hybridization (ISH), immunohistochemistry (IHC) and histological analysis*:** E9-13.5 embryos were immersion-fixed in 4% paraformaldehyde (PFA)/phosphate buffer for 3h. Older embryos were transcardiacally perfused with the same fixative and post-fixed for 2h. Tissue was then washed in phosphate buffer saline (PBS), incubated in a 30% sucrose/PBS solution and embedded and frozen in a 7.5% gelatin in 15% sucrose solution. Cryostat sections were processed for ISH and IHC. ISH were performed with standard protocols. The

following digoxigenin-labeled antisense riboprobes were used: *Dll-1, Hes5, Sfrp1 and Sfrp2*. For BrdU analysis, pregnant mice were injected intraperitoneally with BrdU (50µg/g), sacrificed 1h later and processed for BrdU ICH. ICH analysis was performed as described but sections processed for Otx2, Pax6, Islet-1, phospho-Smad-1,5,8 and NICD were at boiled at 115ºC during 2 min in 10mM citrate buffer using a decloaking chamber (Biocare Medical) for antigen retrieval. NICD IHC was performed as described[19] and amplified with TSA (Perkin Elmer). Immunostaining of the *Drosophila* imaginal discs was performed according to standard protocols and that of extracellular Wg as described in[48]. Fluorescence stained imaginal discs were examined using a confocal laser-scanning microscope (LSM510 Vertical *Zeiss*). We analyzed a minimum of 5 double mutant embryos for each experimental conditions.

Organotypic optic cup cultures. Optic cups from E11.5 mice were dissected embedded in collagen matrices and cultured for 24h in DMEM/F12 medium supplemented with N2 (GIBCO) and different doses of the ADAM10 inhibitor G1254023X re-suspended in DMSO (a gift of Dr. A. Ludwig) or DMSO alone. Cultures were incubated with BrdU (10 µM) for ten minutes before fixation in 4% PFA for 2h. Cultured optic cups were then processed for immunohistochemistry as described above. We analyzed a minimum of 5 optic cups for each experimental conditions.

Overexpression of Sfrp1 and Kuzbanian in Drosophila. Sfrp1 cDNA was fused in frame to a C-terminal Myc tag and cloned into pUAST vector to generate transgenic fly lines expressing SFRP1 under the UAS promoter. The UAS-Kuz was a gift of S. Campuzano. The UAS-Sfrp1 and UAS-Kuz were expressed using the Hh-Gal4 driver[49].

Immunoprecipitations and Western-blot analysis. E13 telencephalic and E15 ocular tissue from wt or Sfrp1/2 null embryos was isolated and homogenized in lysis buffer (150mM NaCl, 2% TritonX-100, 50mM Tris pH 8) containing proteinase and metalloprotease inhibitors (phenanthroline,SIGMA). The lysates were centrifuged for 20 min at 4ºC, the supernatants were precleared in Protein G-Agarose beads (SIGMA-ALDRICH), pre-blocked with 1%BSA for 1h at 4°C and centrifuge at 2000rpm. The supernatants were incubated with anti-Sfrp1 antibody (1µg) overnight at 4°C in a rotor shaker. Protein G-agarose beads were added for 1h, collected by centrifugation at 2000rpm and washed five times with lysis buffer before adding sample buffer without 2-Mercaptoethanol. Beads were boiled for 5 minutes, collected by centrifugation and the supernatants resolved in a 10%SDS-PAGE. Sub-confluent HEK 293T cells were transiently cotransfected with constructs encoding mouse Sfrp1-HA and mouse

ADAM10-myc using the FuGENE HD Transfection Reagent (Roche). After 48h cells were scraped in lysis buffer and immunoprecipitations were performed as described[50]. For sAPP detection, CHO cells were plated in 10-mm dishes in DMEM-F12 10% FCS. After 24 h, cells were incubated with serum-free DMEM in the presence of purified Sfrp1 or Sfrp2. Thereafter cell conditioned media was collected and concentrated on Concanavaline-A beads (GE Healthcare). After electrophoresis, proteins were transferred to PDVF membranes (Hybond-P, Amersham), checked by Ponceau red staining and probed with antibodies against APP (mouse monoclonal anti-Alzheimer precursor protein A4). Western-blot analysis was performed with tissues or cell lines lysed as above. Primary antibodies were detected with peroxidase-conjugated secondary antibodies followed by ECL Advanced Western Blotting Detection Kit (Amersham). Immunoprecipitations and Western blots were repeated at least 3 times obtaining very similar results.

RNA extraction and Q-PCR. mRNA from stage E12.5 and E13.5 embryonic retinas was extracted using the QuickPrep Micro mRNA Purification Kit (GE Healthcare) and treated with DNAse I. cDNAs were obtained by random priming reverse transcription using the First-Strand cDNA Synthesis Kit (GE Healthcare). RT-PCR reactions were run in triplicate in 96-well plates with the SYBR Green PCR Master Mix (Applied Biosystems), using an ABI PRISM 7700 Sequence Detection System (Applied Biosystems). Q-RT-PCR reactions were performed with 3 µl of cDNA, which was used for βactin mRNA amplification for normalization and Hes5 mRNA. Primers were the following *Hes5* forward: 5'-ttcagcaagtgacttctgcga-3', *Hes5* reverse: 5'-tcatagaacccccggtggt-3', βactin forward: 5'-aggtgtgatggtgggaatgg-3', *Dll* forward: 5'-ttgggcttctttaac, Dll-1 reverse: 5'-tccacacactcgttag-3'; *βactin* reverse: 5'-gcctcgtcacccacatagga-3'. Data acquisition and analysis of the real-time RT-PCR assays were performed using the 7500 System SDS Software (v2.0.1, Applied Biosystems). SYBR Green/dsDNA complex signal was normalized to the passive reference dye (ROX) to correct for non-PCR related well-to-well fluorescent fluctuations. Experiments were independently replicated at least three times.

Binding of Sfrp1 to Adam-myc over-expressing CHO line. PCDNA3.1/AP-3myc-Sfrp1 construct was engineered using the PCDNA3.1/AP-3myc plasmid kindly provided by Dr. J. Nathans. HEK293 cells were transiently transfected with PCDNA/AP-3myc-Sfrp1 or PCDNA/AP (alkaline phosphatase) plasmids and conditioned media were recovered after 48h. Control or stably transfected *Adam10* CHO cells were grown in poly-lysine-coated coverslips.

Cells were incubated with conditioned media containing the AP or AP-3myc-Sfrp1 fusion protein for 90m and the detection of bound AP was performed using standard protocols.

Statistical analysis. Normality of the distribution was tested by Kolmogorov-Smirnov test. Statistical significance was determined by T-test. One-way ANOVA was used to compare statistical significance among more than two groups. Post hoc analysis was performed for assessing specific group comparisons (Tukey), when the F value was significant. Values are expressed as means ± standard error of the mean (SEM). Calculations were made using the SPSS statistical package version 17.0 (Chicago, Illinois) using a significance level of 0.05.

Supplementary Information Guide

Figure S1. Sfrp1 and Sfrp2 expression in the retina.
Figure S2. Eye and vasculature formation is disrupted in *Sfrp1*$^{-/-}$*;Sfrp2*$^{-/-}$ embryos.
Figure S3. G1254023X interferes with retinal progenitor proliferation and differentiation.
Figure S4. Proposed model for Sfrp1/2 mechanism of action in the vertebrate eye.

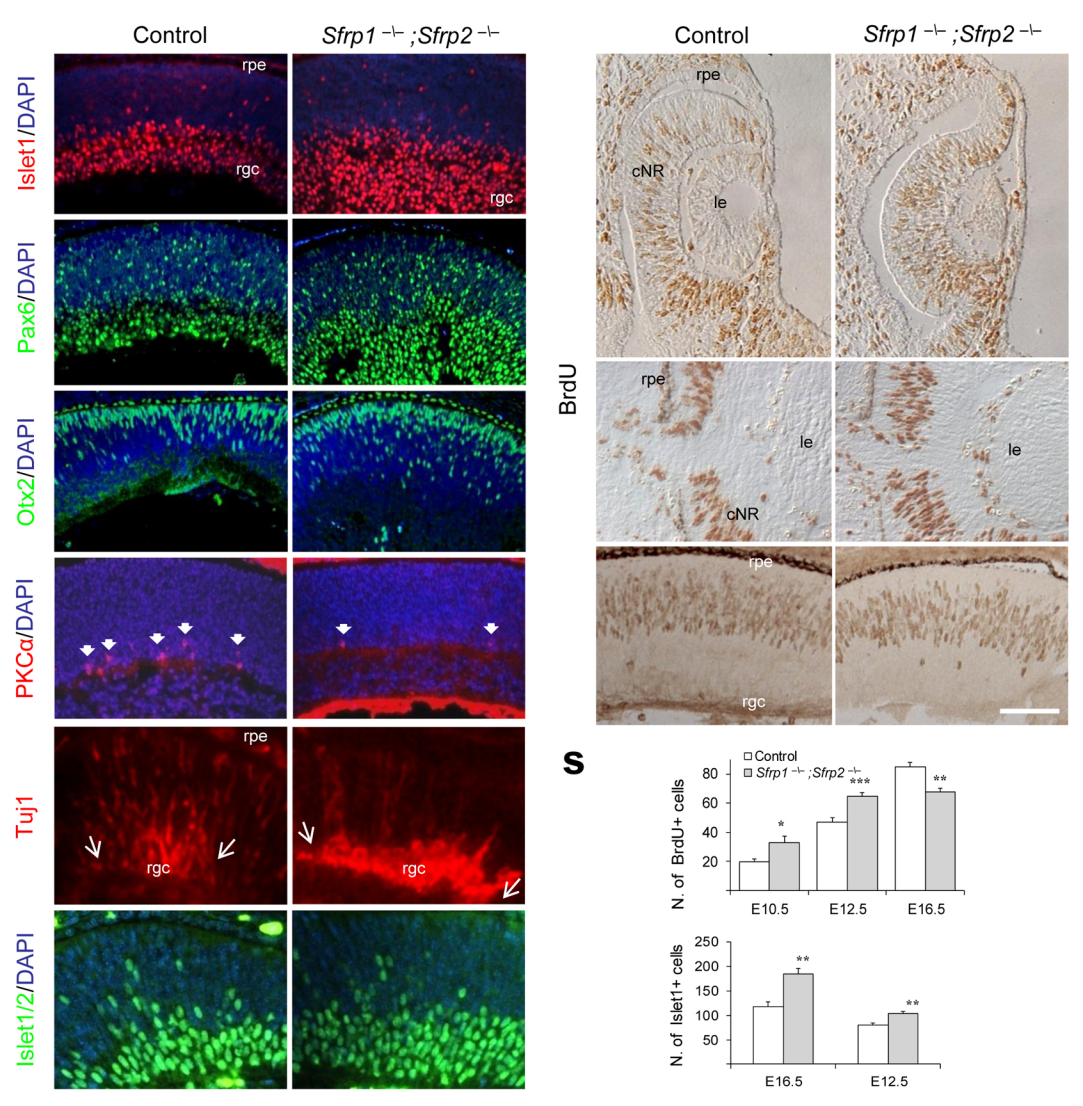
Control
Sfrp1 −/− ;Sfrp2 −/−
Islet1/DAPI
Pax6/DAPI
Otx2/DAPI
PKCα/DAPI
Tuj1
Islet1/2/DAPI
rpe
rgc
cNR
le
BrdU
S
Control
Sfrp1 −/− ;Sfrp2 −/−
N. of BrdU+ cells
E10.5
E12.5
E16.5
N. of Islet1+ cells
E16.5
E12.5

Figure 1

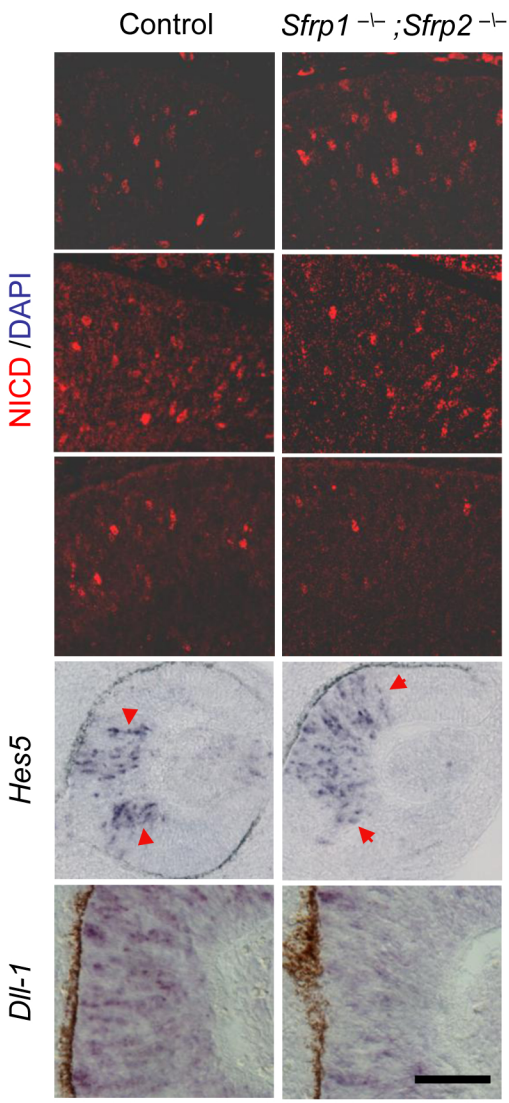
Control
Sfrp1 −/− ;Sfrp2 −/−
NICD /DAPI
Hes5
Dll-1

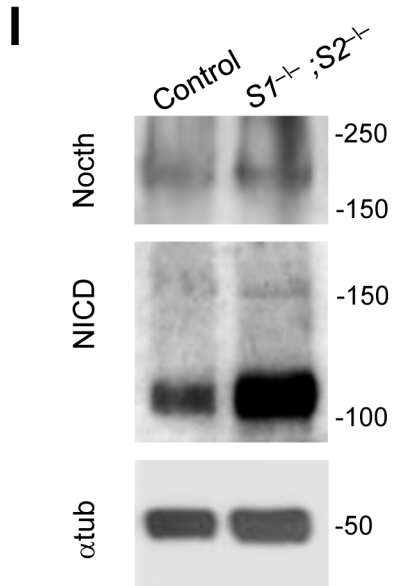
l
Control
S1−/− ;S2−/−
Nocth
NICD
αtub
-250
-150
-150
-100
-50

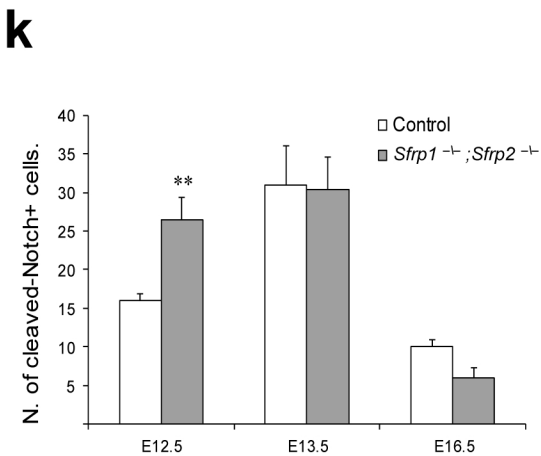
k
N. of cleaved-Notch+ cells.
40
35
30
25
20
15
10
5
**
Control
Sfrp1 −/− ;Sfrp2 −/−
E12.5
E13.5
E16.5

Figure 2

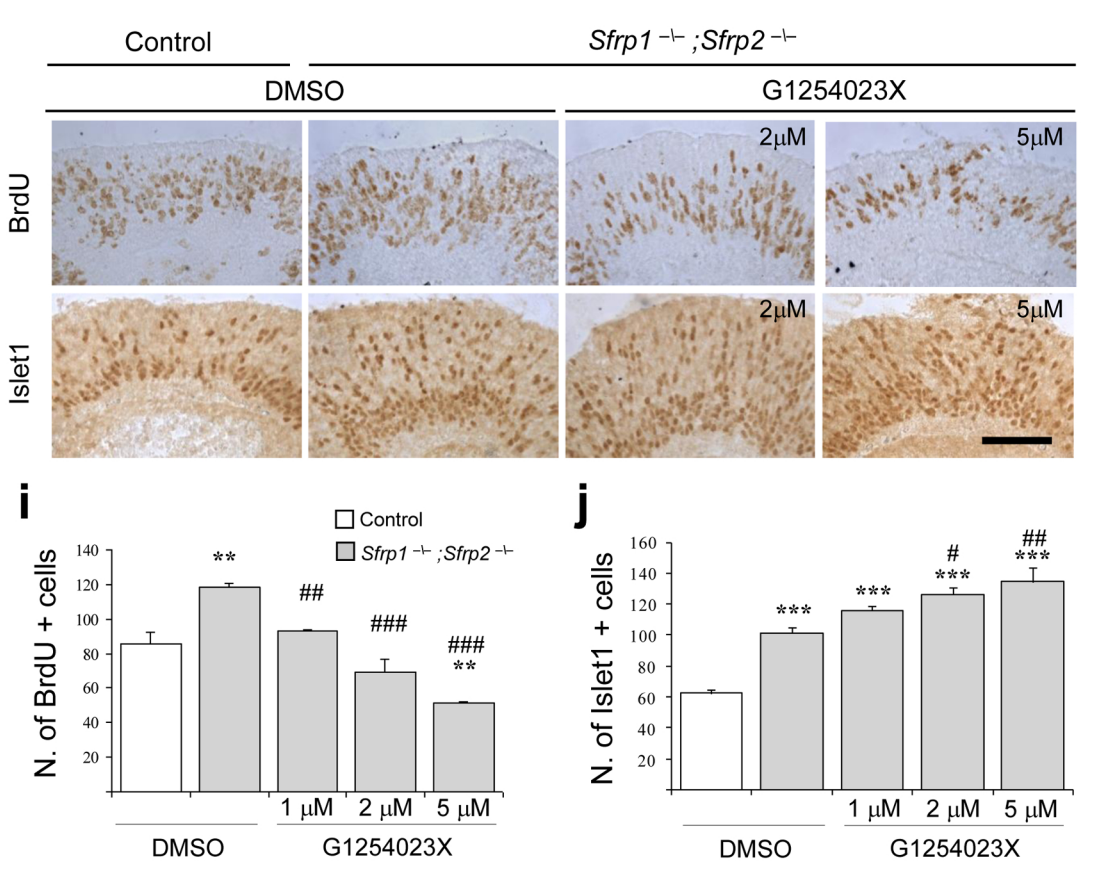
Control
Sfrp1 −/− ;Sfrp2 −/−
DMSO
G1254023X
2μM
5μM
BrdU
Islet1
i
Control
Sfrp1 −/− ;Sfrp2 −/−
N. of BrdU + cells
1 μM
2 μM
5 μM
DMSO
G1254023X
j
N. of Islet1 + cells
1 μM
2 μM
5 μM
DMSO
G1254023X

Figure 3

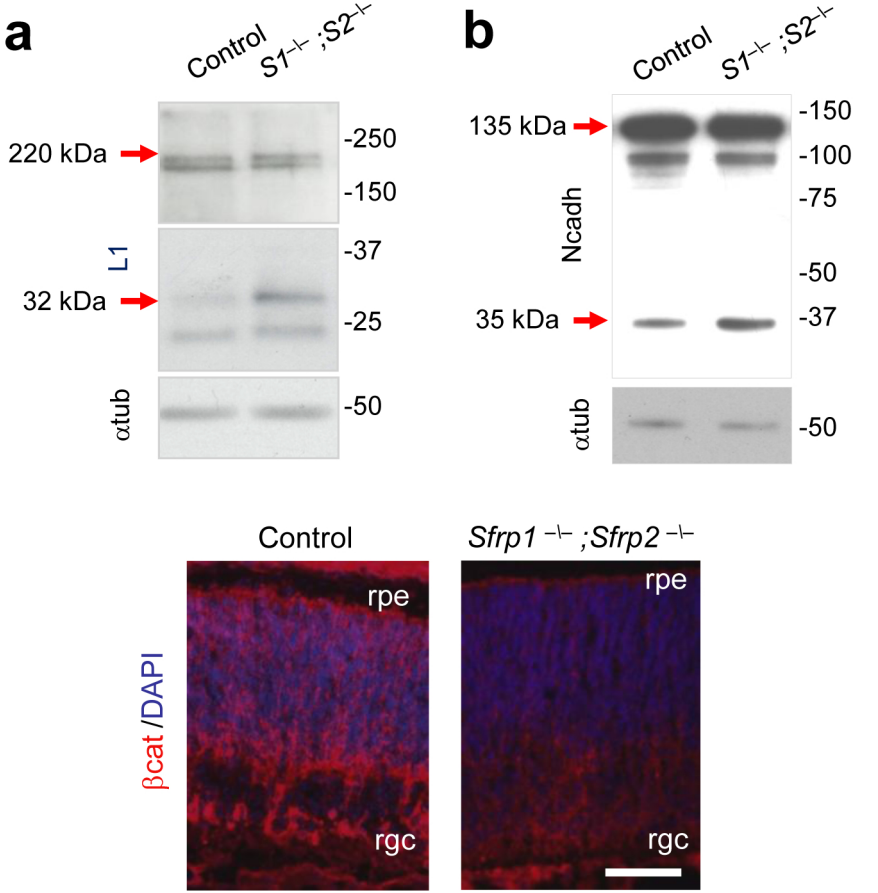
a
Control
S1−/− ;S2−/−
220 kDa
-250
-150
L1
-37
32 kDa
-25
αtub
-50
b
Control
S1−/− ;S2−/−
135 kDa
-150
-100
-75
Ncadh
-50
35 kDa
-37
αtub
-50
Control
Sfrp1 −/− ;Sfrp2 −/−
βcat /DAPI
rpe
rgc
rpe
rgc

Figure 4

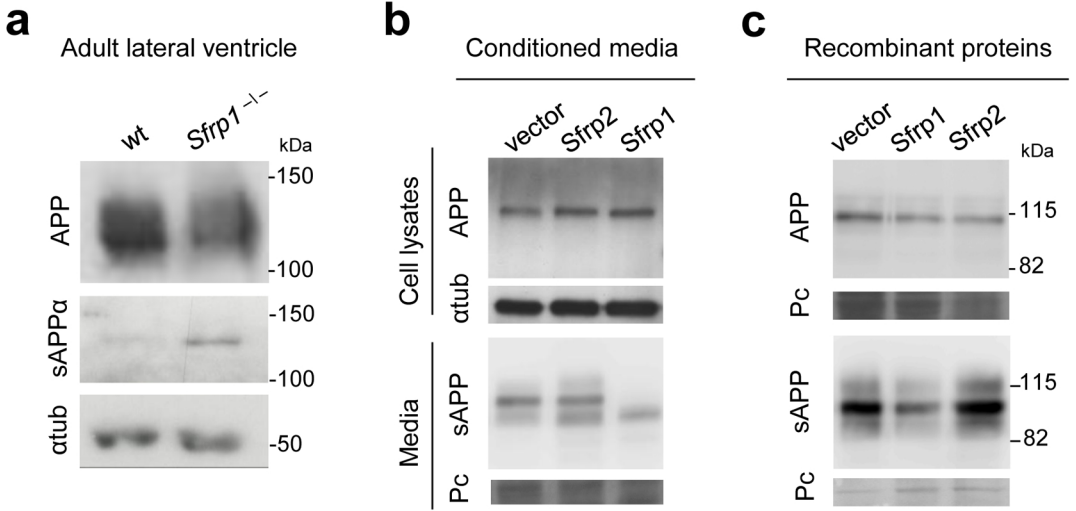
a
Adult lateral ventricle
wt
Sfrp1 −/−
kDa
APP
150
100
sAPPα
150
100
αtub
50
b
Conditioned media
vector
Sfrp2
Sfrp1
Cell lysates
APP
αtub
Media
sAPP
Pc
c
Recombinant proteins
vector
Sfrp1
Sfrp2
kDa
APP
115
82
Pc
sAPP
115
82
Pc

Figure 5

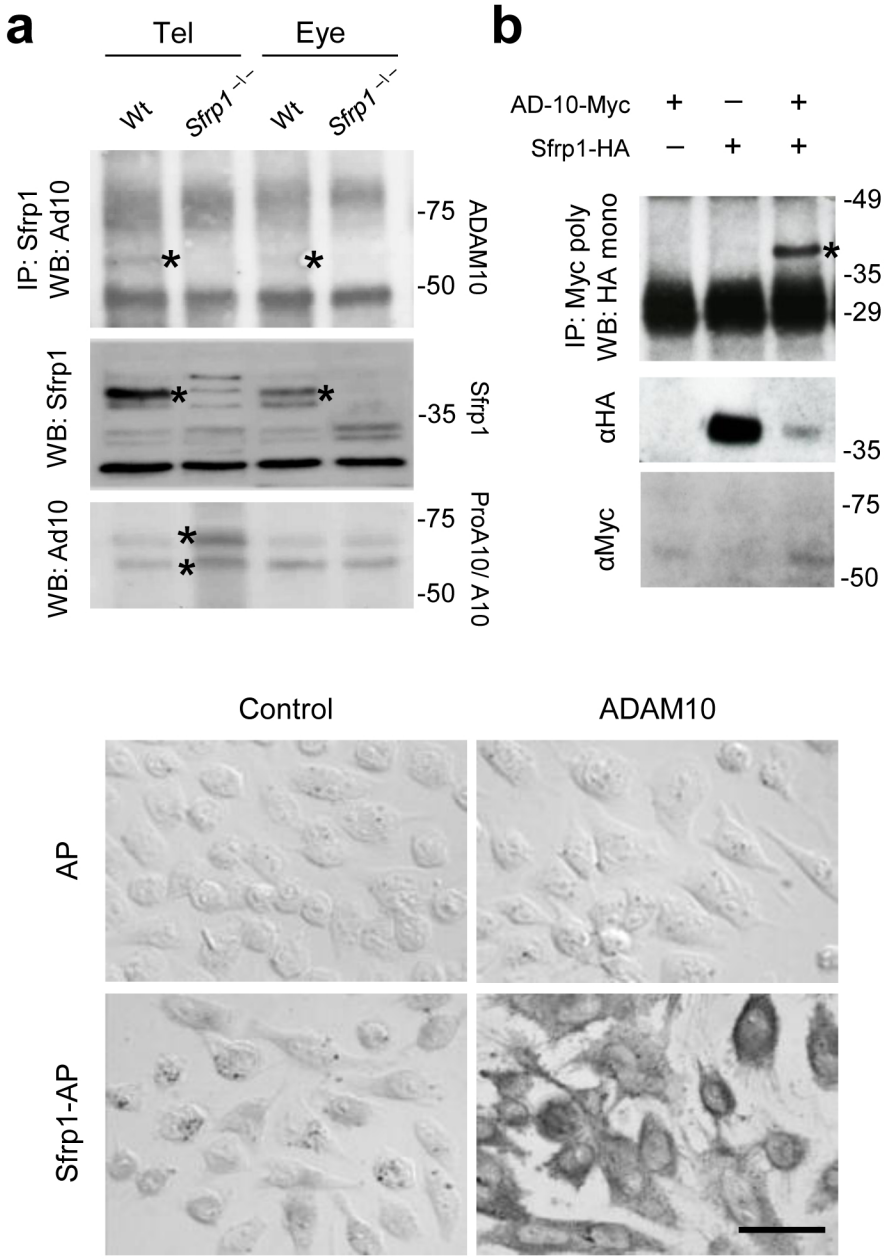
a
Tel
Eye
Wt
Sfrp1 −/−
Wt
Sfrp1 −/−
IP: Sfrp1
WB: Ad10
-75
-50
ADAM10
WB: Sfrp1
-35
Sfrp1
WB: Ad10
-75
-50
ProA10/ A10
b
AD-10-Myc + − +
Sfrp1-HA − + +
IP: Myc poly
WB: HA mono
-49
-35
-29
αHA
-35
αMyc
-75
-50
Control
ADAM10
AP
Sfrp1-AP

Figure 6

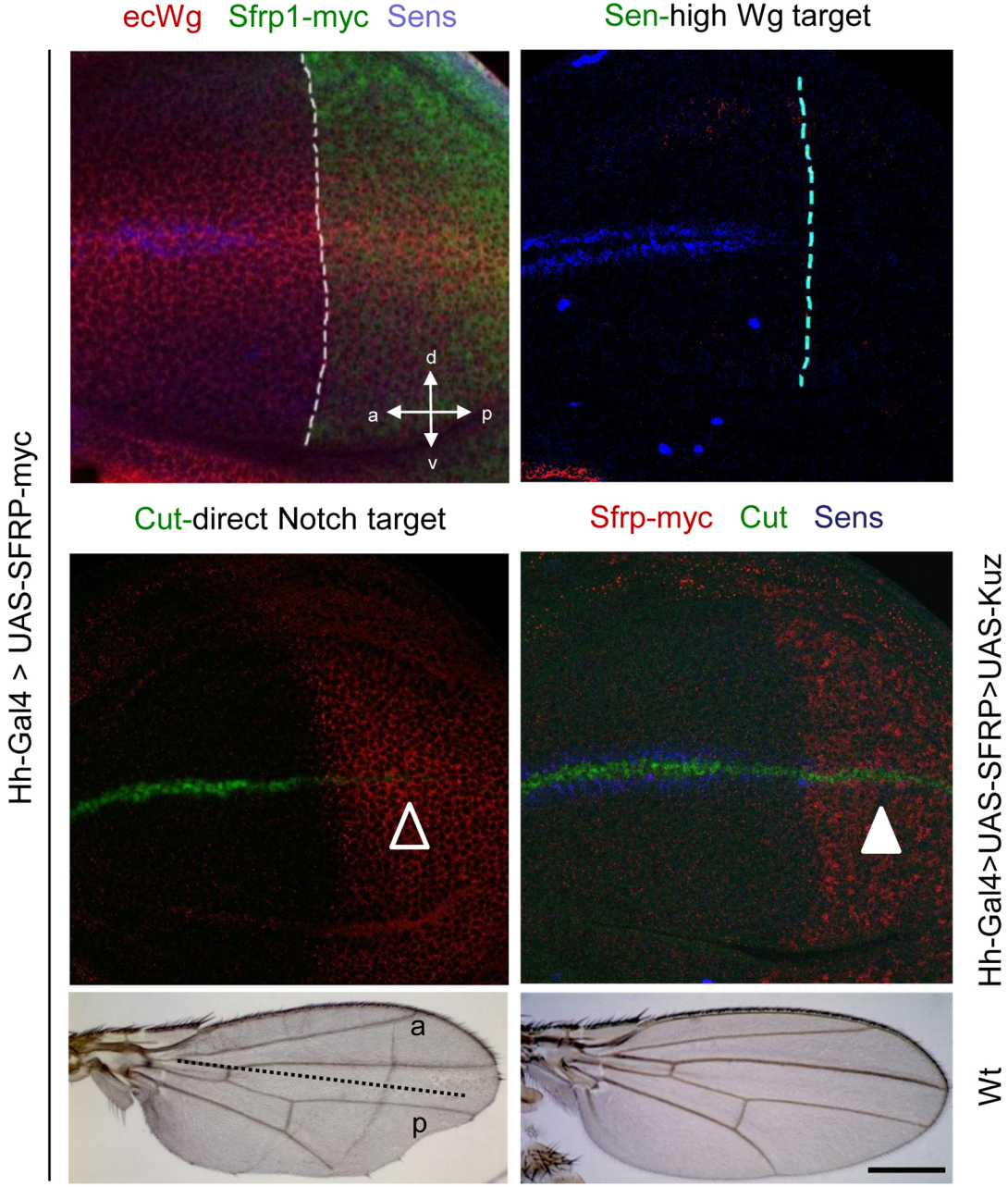
ecWg Sfrp1-myc Sens
Sen-high Wg target
d
a
p
v
Cut-direct Notch target
Sfrp-myc Cut Sens
Hh-Gal4 > UAS-SFRP-myc
Hh-Gal4>UAS-SFRP>UAS-Kuz
a
p
Wt

Figure 7